

Angular dependence of recoil proton polarization in high-energy $\gamma d \rightarrow pn$

X. Jiang,¹ J. Arrington,² F. Benmokhtar,¹ A. Camsonne,³ J.P. Chen,⁴ S. Choi,⁵ E. Chudakov,⁴ F. Cusanno,⁶ A. Deur,⁷ D. Dutta,⁸ F. Garibaldi,⁶ D. Gaskell,⁴ O. Gayou,⁸ R. Gilman,^{1,4} C. Glashauser,¹ D. Hamilton,⁹ O. Hansen,⁴ D.W. Higinbotham,⁴ R.J. Holt,² C.W. de Jager,⁴ M.K. Jones,⁴ L.J. Kaufman,¹⁰ E.R. Kinney,¹¹ K. Kramer,¹² L. Lagamba,⁶ R. de Leo,¹³ J. Leroise,⁴ D. Lhuillier,¹⁴ R. Lindgren,⁷ N. Liyanage,⁷ K. McCormick,¹ Z.-E. Meziani,⁵ R. Michaels,⁴ B. Moffit,¹² P. Monaghan,⁸ S. Nanda,⁴ K.D. Paschke,¹⁰ C.F. Perdrisat,¹² V. Punjabi,¹⁵ I.A. Qattan,^{2,16} R.D. Ransome,¹ P.E. Reimer,² B. Reitz,⁴ A. Saha,⁴ E.C. Schulte,² R. Sheyor,¹⁷ K. Slifer,⁵ P. Solvignon,⁵ V. Sulkosky,¹² G.M. Urciuoli,⁶ E. Voutier,¹⁸ K. Wang,⁷ K. Wijesooriya,² B. Wojtsekhowski,⁴ and L. Zhu⁸

(The Jefferson Lab Hall A Collaboration)

¹Rutgers, The State University of New Jersey, Piscataway, New Jersey 08854

²Argonne National Laboratory, Argonne, Illinois 60439

³Université Blaise Pascal/IN2P3, F-63177 Aubière, France

⁴Thomas Jefferson National Accelerator Facility, Newport News, Virginia 23606

⁵Temple University, Philadelphia, Pennsylvania 19122

⁶INFN, Sezione Sanità and Istituto Superiore di Sanità, Laboratorio di Fisica, I-00161 Rome, Italy

⁷University of Virginia, Charlottesville, Virginia 22901

⁸Massachusetts Institute of Technology, Cambridge, Massachusetts 02139

⁹University of Glasgow, Scotland

¹⁰University of Massachusetts, Amherst, Massachusetts 01003

¹¹University of Colorado, 390 UCB, Boulder, Colorado 80309

¹²College of William and Mary, Williamsburg, Virginia 23187

¹³INFN, INFN/Sezione Bari, Bari, Italy

¹⁴DAPNIA, Saclay, France

¹⁵Norfolk State University, Norfolk, Virginia 23504

¹⁶Northwestern University, Evanston, Illinois 60208

¹⁷University of Tel Aviv, Tel Aviv, Israel

¹⁸Institut des Sciences Nucleaires, Grenoble, France

(Dated: February 8, 2008)

We measured the angular dependence of the three recoil proton polarization components in two-body photodisintegration of the deuteron at a photon energy of 2 GeV. These new data provide a benchmark for calculations based on quantum chromodynamics. Two of the five existing models have made predictions of polarization observables. Both explain the longitudinal polarization transfer satisfactorily. Transverse polarizations are not well described, but suggest isovector dominance.

PACS numbers: 25.20.-x, 24.70.+s, 24.85.+p, 25.10.+s

An important question to nuclear physics is whether one can understand *exclusive* nuclear reactions starting from quantum chromodynamics (QCD), or at least QCD-inspired quark models. Several studies of nuclei [1–4] at high momentum transfer, but in elastic or quasifree kinematics, have shown that the role of explicit quark degrees of freedom is subtle and elusive; even data that probe short ranges can be understood with hadronic theories with the underlying interactions determined from the measured NN force and other inputs. Deuteron photodisintegration is unique among exclusive reactions, in that it has been measured at both large momentum transfer and large energies. Experiments [5–10] have shown that the cross section in the GeV region scales, approximately following the constituent counting rules [11, 12], as would be expected if the underlying dynamics involved quark degrees of freedom. The large energies involve a sum over large numbers of baryonic resonances, leading naturally to the idea of using quark degrees of

freedom to explain the data, although perturbative QCD is not expected to apply [13].

Several quark model calculations [14–18] give competing approximate explanations of the photodisintegration cross sections. All but one are based on the idea that the high energy photon is absorbed by a pair of quarks being interchanged between the two nucleons; the quark-gluon string (QGS) model [15] uses Regge theory to evaluate 3-quark exchange. The models calibrated by the measured NN force [15, 16, 18] tend to better reproduce the cross sections than the models which evaluate the quark-exchange diagram approximately [14, 17]. The reason [17] is that the data scale better with energy than one would expect for the measured energy range.

Polarization observables provide potentially stricter tests of the underlying dynamics [19, 20]. For example, the Σ (linearly polarized photon) asymmetry, measured up to 1.6 GeV, is important for constraining the isoscalar vs. isovector nature of the photon coupling at high en-

ergy [19]. For the recoil proton polarizations, measured at $\theta_{cm} = 90^\circ$ up to 2.4 GeV [22], the induced polarization p_y vanishes, but the polarization transfers $C_{x'}$ and $C_{z'}$ do not, although they are consistent with a slow approach to zero. Thus, while hadron helicity conservation (HHC) [23] does not hold, a slow approach to HHC cannot be ruled out, but it is not expected [24]. Very small induced polarizations, consistent with the data, were predicted by the hard rescattering (HR) model [20], based on modeled pn helicity amplitudes. Here, we present new data at large energy and four-momentum transfer, to further test the theoretical models. These data are the only polarization angular distribution in deuteron photodisintegration measured significantly above 1 GeV.

The experiment (E00-007) ran in Hall A of the Thomas Jefferson National Accelerator Facility (JLab) [25]. A strained GaAs crystal produced the longitudinally polarized electron beam. The beam helicity state was flipped pseudo-randomly at 30 Hz. Beam charge asymmetries between the two helicity states were negligible. The Hall A Møller polarimeter determined the average beam polarization, P_e , to be $76\% \pm 0.3\%$ (statistics) $\pm 3.0\%$ (systematics).

Circularly polarized bremsstrahlung photons were generated when the 2.057-GeV electron beam impinged on a copper radiator with a thickness of 6% radiation length, located 20 cm upstream of the center of a 15-cm liquid deuterium target. The ratio of the photon polarization P_γ to P_e is calculable [26]; here $P_\gamma/P_e \approx 99.5\%$.

Recoil protons from the target were detected in the Hall A left high resolution spectrometer (HRSL) at the five kinematic settings listed in Table I. The scattering angles, momentum, and interaction position at the target were calculated from trajectories measured with Vertical Drift Chambers (VDCs) located in the focal plane. Two planes of plastic scintillators provided triggering and flight time information for particle identification. The incident photon energy was reconstructed from the scattered proton momentum and angle using two-body photodisintegration kinematics. Only events between the bremsstrahlung endpoint and the pion production threshold were used in the analysis.

The final element in the detector stack was the focal plane polarimeter (FPP) [27]. To improve its efficiency, we configured the polarimeter with a dual analyzer system, as in [28]. The VDC chambers, a 44-cm thick polyethylene (CH_2) analyzer, and front straw chambers constituted the first polarimeter, while the front straw chambers, a 49.5-cm carbon analyzer, and rear straw chambers constituted a second, independent polarimeter.

The HRSL spectrometer transverse angle and transverse position resolutions (FWHM) are 2.6 mrad and 4 mm, respectively [25]. Events originating from the target windows were eliminated by cuts on the interaction position. In addition to cuts based on particle's position and direction at the target, a set of 2-dimensional pro-

TABLE I: Kinematics of the data and FPP parameters. A 2 GeV photon energy corresponds to a center of mass energy of $W = 3.3$ GeV.

$\langle E_\gamma \rangle$ GeV	$\langle \theta_{cm}^p \rangle$	$\langle p_p \rangle$ GeV/c	$\langle \theta_{lab}^p \rangle$	spin precession	FPP analyzer	elastic $\vec{e}p$ calibration
2.01	36.9°	2.41	19.8°	226.5°	dual	yes
2.00	52.9°	2.24	29.1°	209.6°	dual	yes
1.99	69.8°	2.01	39.7°	191.9°	dual	yes
1.97	89.8°	1.68	53.9°	167.1°	dual	yes
1.94	109.5°	1.35	70.6°	144.2°	carbon	no

file cuts on the particle position and angle correlations at the focal plane were applied to further eliminate background events. The focal plane profiles were obtained from continuous-momentum spectra taken without the bremsstrahlung radiator. The subtraction of background processes from electro-disintegration used the same techniques as for previous photodisintegration cross-section [5–9] and polarization [22, 29] measurements.

The transverse proton polarization components at the focal plane lead to azimuthal asymmetries in rescattering in the analyzer due to spin-orbit interactions. The alignment of the FPP chambers was determined with straight-through trajectories, with the analyzers removed. Spin transport in the spectrometer was taken into account using a magnetic model calculation. The induced (transferred) polarization was determined by a maximum likelihood method using the sum (difference) of the azimuthal distributions corresponding to the two beam helicity states. If necessary, the proton polarization components obtained in the laboratory frame are transformed into the center-of-mass frame. Previous experiments [22, 27–34] used the same procedures.

TABLE II: The figure of merit (FOM), ϵA^2 , efficiency times analyzing power squared, in %, and the proton form factor ratios obtained from the ep calibration runs. The FOM relative statistical uncertainties are $\approx 15\%$. Statistical uncertainties dominate the form factor ratio uncertainty. $T_{p_{analy}}$, in GeV, is the proton kinetic energy at the mid-point of each analyzer.

p_p^{init} GeV/c	T_p^{init} GeV	CH_2		Carbon		Q^2 GeV ²	$\mu G_E/G_M$
		$T_{p_{analy}}$	FOM	$T_{p_{analy}}$	FOM		
2.41	1.65	1.60	0.41	1.45	0.52	3.10	0.65 \pm 0.11
2.23	1.49	1.45	0.48	1.29	0.69	2.78	0.60 \pm 0.12
2.00	1.28	1.24	0.70	1.08	0.92	2.38	0.79 \pm 0.11
1.68	0.99	0.94	0.99	0.78	1.53	1.85	0.72 \pm 0.05

Calibration runs used $\vec{e}p \rightarrow e\vec{p}$ elastic scattering at 4 GeV for four of the five spectrometer momentum settings of this experiment. Polarization transfer in elastic $\vec{e}p$ scattering determines both the ratio of the proton

electromagnetic form factors [35–38] and the FPP calibration, after accounting for beam polarization and spin transport through the spectrometer; see Table II. Our measurements agree well with previous data for analyzing powers of carbon and CH₂ analyzers [27, 28, 39, 40] and for the form factor ratio [27]. For the γd data at $\theta_{cm}^p = 109.5^\circ$, only the carbon analyzer was used due to the low outgoing proton momentum; the analyzing power was taken from an earlier $\bar{e}p$ calibration run with the same FPP set up [34]. For the four kinematics with dual analyzers, recoil polarizations were consistent between the two analyzers within uncertainties, and the weighted averages are given as the final results in Table III.

TABLE III: Center-of-mass frame proton recoil polarization components, with statistical and systematic uncertainties.

θ_{cm}^p	p_y	$C'_{x'}$	$C'_{z'}$
36.9°	-0.301 ± 0.053 ± 0.029	-0.170 ± 0.041 ± 0.020	0.654 ± 0.056 ± 0.051
52.9°	-0.209 ± 0.041 ± 0.052	-0.205 ± 0.040 ± 0.031	0.573 ± 0.071 ± 0.092
69.8°	0.008 ± 0.033 ± 0.039	-0.228 ± 0.045 ± 0.033	0.835 ± 0.108 ± 0.116
89.8°	-0.090 ± 0.049 ± 0.045	0.065 ± 0.074 ± 0.034	0.453 ± 0.162 ± 0.065
109.5°	0.226 ± 0.073 ± 0.053	0.316 ± 0.082 ± 0.035	0.001 ± 0.119 ± 0.037

There are several systematic uncertainties. The statistical uncertainties of the measured analyzing powers dominate over the beam polarization uncertainty. Spectrometer offsets also contribute. Potential geometrical biases are eliminated by requiring that all possible secondary scattering proton azimuthal angles (ϕ_{FPP}) fall into the boundaries of the polarimeter. The induced polarization p_y in ep elastic scattering vanishes – neglecting small effects from two-photon exchange – allowing a direct measurement of the false asymmetries in the polarimeter. The ep induced polarization measurements were all consistent with vanishing, so the statistical accuracies of p_y in the ep calibration (≤ 0.04), were assigned as the false asymmetry systematic uncertainties of the induced polarization in deuteron photodisintegration. For the polarization transfer, the false asymmetries largely cancel in forming the helicity differences.

Figure 1 compares the proton recoil polarization of this work (E00-007), at $E_\gamma \approx 2$ GeV, with earlier results (Wijesooriya) [22] at $E_\gamma = 1.86$ GeV, and calculations. A slow energy dependence of the recoil polarizations above $E_\gamma \approx 1$ GeV was found in [22], and our new measurements at $\theta_{cm} = 90^\circ$ are compatible with the earlier results. All three polarization components are consistent with a smooth variation with angle, and with crossing

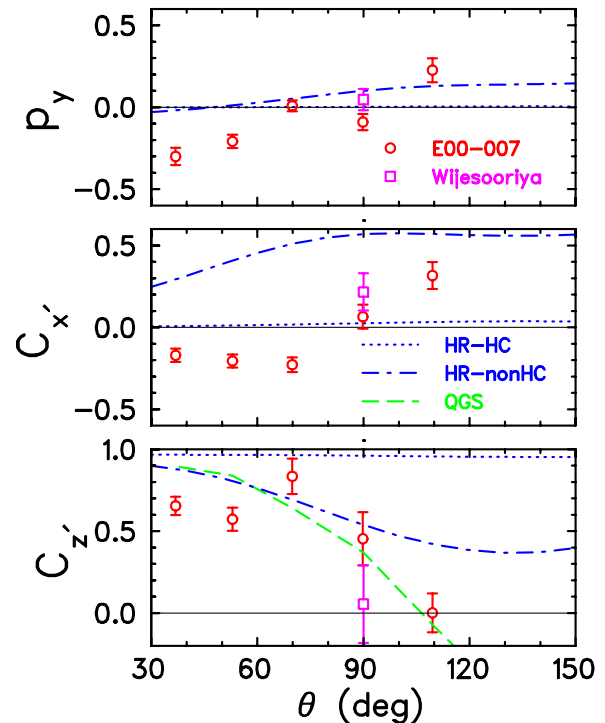


FIG. 1: (Color online) Polarization transfers $C'_{x'}$, $C'_{z'}$ and induced polarization p_y in deuteron photodisintegration. Only statistical uncertainties are shown. See text for details.

zero near $\theta_{cm} = 90^\circ$. Both $C_{x'}$ and p_y start out negative and moderately sized at forward angles, while $C_{z'}$ is positive and large. As p_y and $C_{x'}$ do not generally vanish, we again confirm that HHC does not hold.

The longitudinal polarization is given by [41]

$$f(\theta)C_{z'} = \sum_{i=1}^6 \sum_{\pm} \pm |F_{i,\pm}|^2, \quad (1)$$

with $f(\theta)$ the cross section. It is insensitive to phases of amplitudes. Except for the negative signs, $C_{z'}$ would equal the cross section, and could be predicted as reliably. In contrast, $C_{x'}$ and p_y are the real and imaginary parts of the same sum of interfering amplitudes [13, 41], and are highly sensitive to phases, and difficult to predict.

Two calculations of the spin observables are available. Figure 1 shows that the QGS model [19] predicts a longitudinal polarization transfer in good qualitative agreement with the measured data, but makes no prediction for the transverse polarizations, due to their sensitivity to phases. Given the good agreement with deuteron photodisintegration cross sections in the few GeV region [10], the QGS model must be regarded as the most successful existing model of photodisintegration at a few GeV.

Figure 1 also shows predictions for all three observables from the HR model [20]. It should be noted that these calculations are at the lower edge of the nominal validity range of the model. Also, since the pn spin amplitudes

are not well constrained by data, the pn amplitudes are based on pp data. Thus, there are large uncertainties in the predictions. One calculation (dotted line) assumes that there is only small helicity nonconservation, leading to small values of $C_{x'}$ and p_y , and $C_{z'}$ being nearly unity [43]. The second (dash-dot line) calculation assumes large helicity non-conservation. The comparison with all observables supports large helicity nonconservation, but clearly the predictions for the transverse polarization are not in sufficiently good agreement. However, ref. [20] points out that the transverse polarizations are approximately proportional to a particular amplitude in pn scattering (“ ϕ_5 ”) that vanishes at $\theta_{cm} = 90^\circ$ in the isovector channel. Thus, the transverse polarization data might be indicating that the isovector channel dominates over the isoscalar channel, more so than in the calculation. This observation is consistent with the situation in the Σ asymmetry, mentioned above. While the HR model does not agree quite as well as the QGS model with $C_{z'}$ or with the cross sections for energies around 2 GeV, it is at least as successful at predicting cross section above about 3 GeV [13], and its p_y predictions are consistent with the large-angle data.

To summarize, we provide new benchmark data for polarizations in deuteron photodisintegration. The two models which predict the longitudinal polarization transfer, the QGS and HR models, are in qualitative agreement with these data; while neither model adequately explains the transverse polarizations, the HR model indicates the qualitative behavior might arise from isovector dominance. High-energy photodisintegration of pp pairs [42] is the next major test of the underlying dynamics and of the theoretical models, as these two models give very different predictions for pp photodisintegration.

We thank Drs. Brodsky, Grishina, Hiller, Lee, Kondratyuk, Miller, Radyushkin, Sargsian and Strikman for many interesting discussions. We thank the JLab physics and accelerator divisions for their support, particularly the cryotarget and Hall A technical staffs for their extensive support at short notice. This work was supported by the U.S. National Science Foundation, the U.S. Department of Energy, and the Italian Istituto Nazionale di Fisica Nucleare. The Southeastern Universities Research Association (SURA) operates the Thomas Jefferson National Accelerator Facility under DOE contract DE-AC05-84ER40150. The polarimeter was funded by the U.S. National Science Foundation, grants PHY 9213864 and PHY 9213869.

[1] L.C. Alexa *et al.*, Phys. Rev. Lett. **82**, 1374 (1999).
 [2] D. Abbott *et al.*, Phys. Rev. Lett. **84**, 5053 (2000).
 [3] F. Benmokhtar *et al.*, Phys. Rev. Lett. **94**, 082305 (2005).
 [4] M. Rvachev *et al.*, Phys. Rev. Lett. **94**, 192302 (2005).
 [5] J. Napolitano *et al.*, Phys. Rev. Lett. **61**, 2530 (1988);

S.J. Freedman *et al.*, Phys. Rev. C **48**, 1864 (1993).
 [6] J.E. Belz *et al.*, Phys. Rev. Lett. **74**, 646 (1995).
 [7] C. Bochna *et al.*, Phys. Rev. Lett. **81**, 4576 (1998).
 [8] E.C. Schulte *et al.*, Phys. Rev. Lett. **87**, 102302 (2001).
 [9] E.C. Schulte *et al.*, Phys. Rev. C **66**, 042201R (2002).
 [10] M. Mirazita *et al.*, Phys. Rev. C **70**, 014005 (2004).
 [11] S.J. Brodsky and G.R. Farrar, Phys. Rev. Lett. **31**, 1153 (1973); V. Matveev *et al.*, Nuovo Cim. Lett. **7**, 719 (1973).
 [12] P. Rossi *et al.*, Phys. Rev. Lett. **94**, 012301 (2005).
 [13] R. Gilman and Franz Gross, J. Phys. G **28**, R37 (2002).
 [14] S.J. Brodsky and J.R. Hiller, Phys. Rev. C **28**, 475 (1983).
 [15] E. De Sanctis *et al.*, Few Body Syst. Suppl. **6**, 229 (1992); L. A. Kondratyuk *et al.*, Phys. Rev. C **48**, 2491 (1993); V.Yu Grishina *et al.*, Eur. Phys. J. A **10**, 355 (2001).
 [16] L.L. Frankfurt, G.A. Miller, M.M. Sargsian, and M.I. Strikman, Phys. Rev. Lett. **84**, 3045 (2000); L.L. Frankfurt, G.A. Miller, M.M. Sargsian, and M.I. Strikman, Nucl. Phys. A **663**, 349 (2000).
 [17] A. Radyushkin, private communication.
 [18] B. Julia-Diaz and T.-S. H. Lee, Mod. Phys. Lett. A **18**, 200 (2003).
 [19] V.Yu Grishina *et al.*, Eur. Phys. J. A **18**, 207 (2003); V.Yu Grishina *et al.*, Eur. Phys. J. A **19**, 117 (2004).
 [20] M.M. Sargsian, Phys. Lett. B **587**, 41 (2004).
 [21] F. Adamian *et al.*, Eur. Phys. J. A **8**, 423 (2000).
 [22] K. Wijesooriya *et al.*, Phys. Rev. Lett. **86**, 2975 (2001).
 [23] See S.J. Brodsky and G.P. Lepage, Phys. Rev. D **24**, 2848 (1981), and references therein.
 [24] T. Goussset, B. Pire, and J.P. Ralston, Phys. Rev. D **53**, 1202 (1996).
 [25] J. Alcorn *et al.*, Nucl. Instrum. Methods A **522**, 294 (2004).
 [26] H. Olsen and L. C. Maximon, Phys. Rev. **110**, 589 (1958).
 [27] V. Punjabi *et al.*, Phys. Rev. C **71**, 055202 (2005); Publisher’s Note Phys. Rev. C **71**, 069902 (2005).
 [28] D. J. Hamilton *et al.*, Phys. Rev. Lett. **94**, 242001 (2005).
 [29] K. Wijesooriya *et al.*, Phys. Rev. C **66**, 034614 (2002).
 [30] M.K. Jones *et al.*, Phys. Rev. Lett. **84**, 1398 (2000);
 [31] O. Gayou *et al.*, Phys. Rev. C **64**, 038202 (2001).
 [32] O. Gayou *et al.*, Phys. Rev. Lett. **88**, 092301 (2002).
 [33] S. Strauch *et al.*, Phys. Rev. Lett. **91**, 052301 (2003).
 [34] J. J. Kelly *et al.*, Phys. Rev. Lett. **95**, 102001 (2005).
 [35] A.I. Akhiezer and M.P. Rekalo, Sov. Phys. Doklady **13**, 572 (1968).
 [36] N. Dombey, Rev. Mod. Phys. **41**, 236 (1969).
 [37] A.I. Akhiezer and M.P. Rekalo, Sov. J. Part. Nucl. **3**, 277 (1974).
 [38] R. Arnold, C. Carlson and F. Gross, Phys. Rev. C **23**, 363 (1981).
 [39] M.W. McNaughton *et al.*, Nucl. Instrum. Methods A **241**, 435 (1985).
 [40] N.E. Cheung *et al.*, Nucl. Instrum. Methods A **363**, 561 (1995); B. Bonin *et al.*, Nucl. Instrum. Methods A **288**, 379 (1990).
 [41] V.P. Barannik *et al.*, Nucl. Phys. A **451**, 751 (1986).
 [42] S.J. Brodsky *et al.*, Phys. Lett. B **578**, 69 (2003); E. Piasetzky *et al.*, Jefferson Lab proposal E03-101.
 [43] Helicity conservation leads to $C_{x'}$ and p_y vanishing, but the limit for $C_{z'}$ is model dependent. In the HR model, the helicity conserving amplitude $F_{1+} \geq F_{5\pm}$, while F_{3-} is small, as a + helicity photon scatters from a + helicity proton. The limit is *not* the same as the usual one

presented in [13], which assumes $F_{1+} \approx F_{3-}$.